EACWE 5
Florence, Italy
19th – 23rd July 2009

Flying Sphere image © Museo Ideale L. Da Vinci

The Solar Updraft Power Plant: Design and Optimization of the Tower for Wind Effects

H.-J.Niemann[1)], F.Lupi[2)], R.Hoeffer[3)], W.Hubert[1)], C. Borri[2)]
[1)] Niemann & Partner Consultants – Niemann@IGNundP.de – Universitaetsstrasse 142, D-44799 Bochum – [2)] Università degli Studi di Firenze – francescalupi@alice.it – 501139 Firenze – [3)] Ruhr-Universitaet Bochum – ruediger.hoeffer@rub.de – D-44780 Bochum

Keywords: ultra-high towers, wind at high altitudes, mean and fluctuating wind load, structural optimization for wind induced stresses

ABSTRACT

Solar updraft power generation has first been proposed in 1903 by the Spanish engineer I. Cabanyes, followed by a description by the German scientist [Günther 1931]. Starting in 1982, a team with the German civil engineer J. Schlaich constructed a prototype solar udraft power plant (SUPP) in Manzanares, Spain, with a 200 m high solar chimney (SC) and a maximum power output of 50 kW. This prototype plant operated successfully for more than 6 years. It provided basic figures for all future developments. Since those days, several projects for SUPPs have been planned in the world's arid zones, but none of them has been brought to realization, up to now.

The chimney dimensions range from 1000 m in height and 150 m in tip diameter up to 1500 m in height and a tip diameter of 170 m depending on the required power output of 100 to 400 MWp. The SC is basically a circular cylindrical or, similar to Natural Draught Cooling Towers, a hyperbolic tower, or a mixture of both. It is designed as a concrete shell structure. Stiffening rings are applied at the top and at various levels along the height in order to stabilize its cross-section.

From all actions, the actions of the wind play the most important role in the SC-, but as well in the CA-design. They dominate largely the costs and thus decide on the economic feasibility of the SUPP technology.

Contact person: 1st H.-J. Niemann, Niemann & Partner Consultants, Technologiezentrum Ruhr, Universitaetsstr. 142, D-44799 Bochum, Tel. 49 234 9048680, FAX 49 234 9048689 E-mail Niemann@IGNuP.de

The wind load effects may be diminished by optimizing the structural behaviour of the tower. The nature of the wind at high altitudes, the aerodynamic loads, the amount of resonant response, and the structural optimization are discussed in the present paper.

1. INTRODUCTION

The general working principle of a SUPP is illustrated in figure 1. Such power plants consist of the collector area, the turbine(s) with coupled generator(s) as power conversion unit, the solar chimney and the electrical equipment. In the collector, a large glass-covered area, solar irradiation heats the collector ground and consequently warms up the air inside the collector area. Following the increasing height of the roof, the heated air streams towards the chimney at the collector centre, and fresh cold air is drawn into the collector at its perimeter slot. In the power conversion unit at the solar chimney foot, the mass stream of warm air is transformed into kinetic and further into electric power.

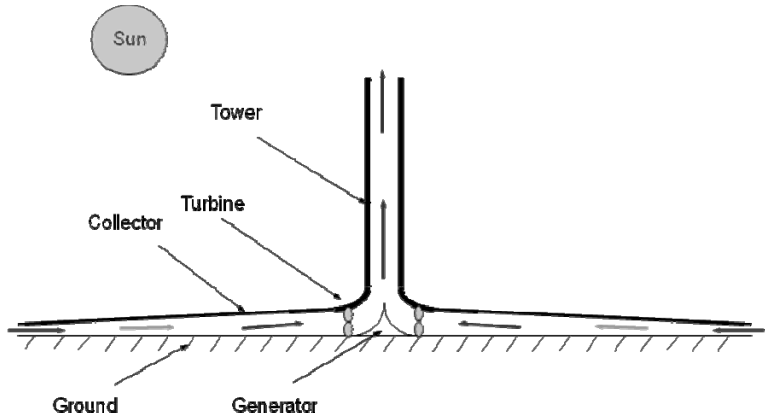

Figure 1: Schematic of a Solar Updraft Power Plant

Solar updraft power plants are the most sustainable natural resources for electric power generation. During service, they are completely free of carbon-dioxide emissions, since they use solar irradiation as fuel. If one incorporates all materials required for the plant construction in an energy balance, measured by CO_2-emissions, one ends up with around ≈10 g of CO_2 per kWh of produced electric work, depending on the service life-duration of the plant. Since design service-lives are 80 to 120 years, CO_2-emissions and production costs of the electric current are by far the smallest ones of all renewable energies even if renewals of the turbo-generators and parts of the glass-roof are included.

Solar chimneys as dominant structures of SUPPs are exposed to characteristic actions such as:

1. Dead weight D, mainly from the self-weight of the shell wall (25.0 kN/m³);
2. Wind loading W consisting of the external pressure distribution and the internal suction;
3. Dynamic along wind load due to wind gustiness, and cross wind loading caused by regular periodic vortex separation;
4. Temperature effects T from actions of the heated air on the RC wall;
5. Shrinkage effects S in the (fresh) RC shell may lead to cracking by residual stress states;
6. Differential soil settlements B of external origin;
7. Seismic actions E, if the location of the SUPP owns a sufficient seismicity;
8. Construction loads M mainly from pre-stressed guys of the central tower crane.

From all these actions, wind effects play the most important role in the tower design. They dominate largely the tower costs and thus decide on the economic feasibility of the SUPP technology.

The tower height is beyond present experience. Simplified models for the wind action which provide safe and economic structures when the tower height is limited to 300 m, are no longer applicable. The wind flow in the atmospheric boundary layer beyond 300 m, in particular its turbulence must be reconsidered since detailed experimental evidence does not go further up than that level.

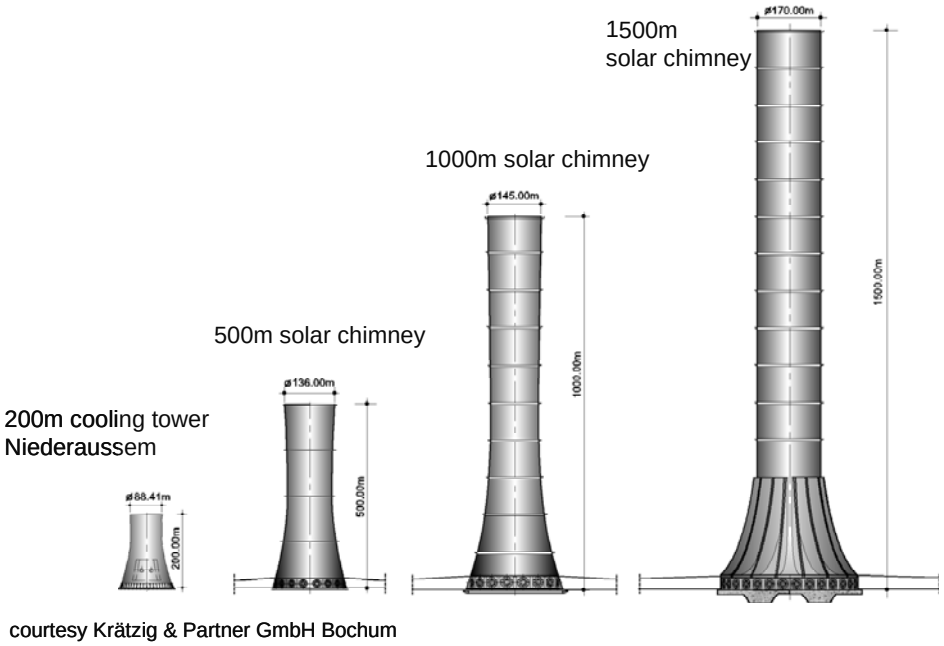

Figure 2: Three Variants of Solar Chimneys

2. THE DESIGN WIND SPEED IN VIEW OF STRUCTURAL RELIABILITY OF THE SOLAR CHIMNEY

In the tower design, the safety concept combines internal forces computed from the characteristic loads for recommended load combinations such that sufficient safety is guaranteed. Since there do not exist special regulations for RC shell structures of such an extreme height, we base our designs on the German cooling tower code [VGB-650 Ue], which is in agreement with the European Standards EC 1, 2 and the German guide lines DIN 1055-100, DIN 1045-1. Limit states of failure and of serviceability are considered, in which permanent, temporary and frequent design situations are distinguished. Starting for a given thickness distribution with a linear-elastic analysis of the entire chimney, the reinforcement under the leading action of the wind is determined in the ultimate limit state from the load combination:

$$\gamma_D D + \gamma_W W + \psi_{0B}\gamma_B B + \psi_{0S}\gamma_S S \qquad (1)$$

The partial factors and combination factors are specified in the guideline [VGB-650 Ue] as:
γ_D = 1.0/1.35 (favourable/unfavourable);
γ_W = 1.6;
γ_B = 0/1.5 (favourable/unfavourable);
γ_T = 0/1.5 (favourable/unfavourable);
$\psi_{0B} = \psi_{0S}$ = 1.0

The partial factor for the design wind load depends on the level of reliability considered. For example, the Eurocode [EN 1990] "Basis of design" specifies a target maximum of the failure probability of $P_f = 1.25\ 10^{-6}$ related to one year, corresponding to $P_f = 7.2\ 10^{-5}$ in the design working life of 50 yrs. Corresponding values of the minimum reliability index are $\beta = 4.7$ (1 yr) and $\beta = 3.8$ (50 yrs). All these targets are notional, intended primarily as a tool for developing consistent design rules. The relation between P_f and β is given by $P_f = \Phi(-\beta)$, in which Φ is the standard Gauss probability function. The related probability of exceeding the design value of an action effect, E_d, in the ultimate limit state of structural failure, is somewhat higher and calculated from $P(E>E_d) = \Phi(\alpha_E \cdot \beta)$ in which α_E is the participation factor of the load considered, $-1 \le \alpha_E < 0$. Given the exceedance probability, the design wind speed can be calculated from an appropriate extreme value probability function of yearly maxima of mean wind speeds. For practical reasons, the design

wind speed is related to a reference or so-called characteristic wind speed which has a return period of 50 yrs. The ratio of design to characteristic wind loads is the partial safety factor. Since the wind load is proportional to the square of the wind speed, the partial factor of the wind load is the square of the ratio of the design wind speed to the characteristic wind speed.

The result of this operation depends much on the type of probability distribution fitted to observed statistical wind data. The Eurocode 1990 recommends a partial factor of $\gamma_W = 1.5$ based on the Gumbel type I probability distribution. It is valid for most non-permanent loads in general. Applying the procedure to the wind loading problem, it is generally assumed that the Gumbel I distribution applies to the statistics of mean wind speeds. The following table shows the partial wind load factor calculated for different probability functions and participation factors. The first two applications rely on the Gumbel type I distribution.

Type of Gumbel distribution	α_W	β_1	$\Phi(\alpha_w \cdot \beta_1)$	V_V	γ_W
I	-0.7	4.7	4.5^{-4}	0.12	1.5 - 1.6
I	-1.0	4.7	1.25^{-6}	0.12	2.0
III	-1.0	4.7	1.25^{-6}	0.12	1.4

Table 1: Partial factor for the wind load for different probability functions

The first line relates to a case, where the wind load is the leading action in a combination with others. The partial factor is close to the code specification. The second line is a limiting, rather unrealistic case where all design variables other than the wind load are deterministic. The partial factor will always be lower than this value. The type I distribution has neither lower nor upper limits. Obviously, there must be an upper limit to the wind velocity. The Gumbel type III distribution includes this option. Wind data from ca. 60 meteorological stations all over Germany have been analyzed to estimate the upper limit in relation to the individual mean and standard deviation; [Niemann et al 2007]. The result of this investigation is a partial factor of 1.4 shown in the third line. It indicates that the standard load factor is on the safe side and may eventually be reduced without any loss in target reliability.

3. MEAN WIND AND TURBULENCE BEYOND THE PRANDTL LAYER

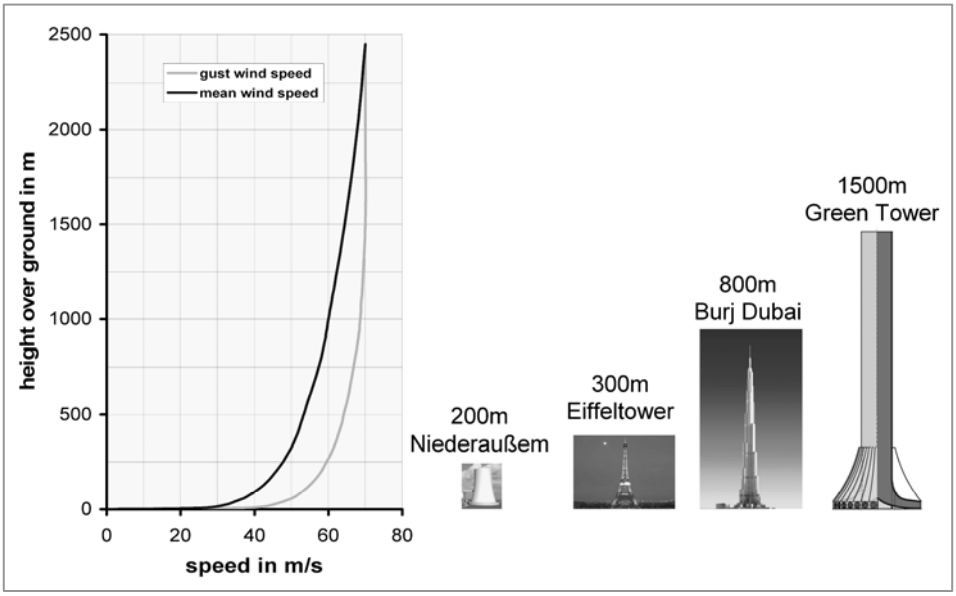

Figure 3: Profiles of mean and gust wind speed

Prandtl's constant shear concept for boundary layers in fluid dynamics, describes the natural wind flow up to 70 - 100 m distance to the ground correctly. It is adequate for wind loads on structures,

extending to a height of up to 300°m. The mean wind profile specifies the mean wind load, whereas the turbulence parameters (intensity, integral length scales as a measure of correlation, and spectral density) provide the input to the dynamic load. Solar chimneys reach far beyond the Prandtl layer into the Ekman layer. Here, the shear and the turbulence decrease, whereas the Coriolis force becomes important. It increases the mean wind speed compared to the logarithmic law. The difference between gust and mean wind speed vanishes asymptotically as the height above ground increases, see fig. 2. A 1500 m tower approaches even the height of the ABL thickness $z = \delta$, where the ABL ends and the geostrophic wind flow prevails. At $z \geq \delta$, the shear is negligible and the dynamic load component vanishes. In the Ekman layer, experimental meteorological data are scarce. However, theoretical considerations provide models for the mean and fluctuating wind components, see e.g. [Harris and Deaves 1980]. The model refers strictly to neutral thermal stratification. In non-neutral conditions, downbursts increase the peak gust velocity [Bradbury et al 1994] and may become important for the collector glass roof. This question needs further attention.
The material properties of the fluid, especially its density $\rho = \rho(z)$ but as well the viscosity, vary over the tower height. At 1500m above ground the mass density is 87% of its value at ground level. The wind load decreases accordingly.

4. WIND LOADING

4.1 Mean wind load

The mean wind load is represented by pressure differences resulting from a uniform negative pressure inside the tower and the external pressure distribution. The latter depend on Reynolds number and on the roughness of the exterior surface. The load distributions developed for NDCTs since the mid 1960s [Niemann 1993] apply also to the Solar Chimney, with two exceptions:
(1) In the tip region, the pressures deviate from the typical circumferential distribution observed at lower levels at the tower height. Due to the higher slenderness of SCs compared to NDCTs, this so-called tip effect extends over a larger part of the tower height and must be taken into account.
(2) High surface roughness reduces the suction peaks at the tower sides. At the same time, the overall wind force increases with high surface roughness, see fig. 3. Due to the load carrying behaviour of NDCTs, small suction induces small tensile meridional stresses in the shell. For this reason, wind ribs are commonly applied at the exterior surface of cooling towers. For SCs however, another effect of their higher slenderness is that the stress distribution comes closer to a beam. The stiffening of the SC shell by a number of rings increases this tendency. In such a case, the stresses are the smaller, the smaller the overall wind force is. Now, the smooth surface becomes the optimal solution for SCs.

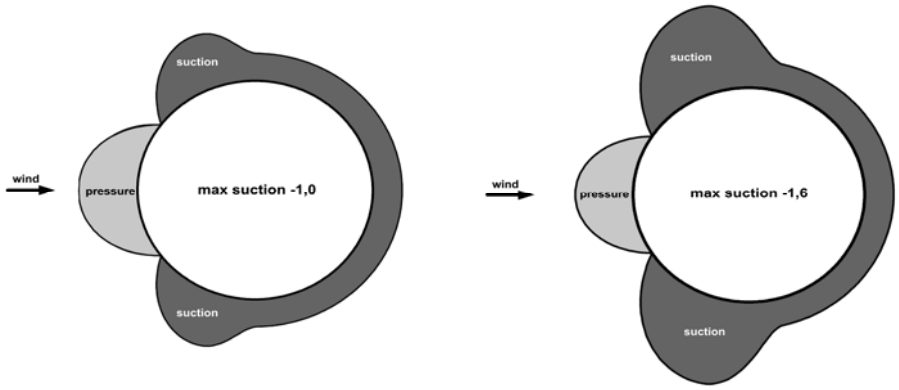

Figure 4: Pressure distribution outside the tip region; a) tower surface with wind ribs, aerodynamic drag coefficient 0.66; b) smooth tower surface, aerodynamic drag coefficient 0.46

The calculation method for the mean wind load effects (stresses, deflections) is well established in practical design. This does not apply to the effects of the fluctuating wind load.

4.2 Response to wind turbulence

The response to wind turbulence must be considered in terms of its standard deviation. It has two components: (1) the response to background turbulence which goes without resonance and includes the lack of correlation of the pressure fluctuations on the shell surface; (2) the resonant response which is caused by turbulence in resonance with vibration modes. The resonant component is small if the natural frequency of the excited mode is sufficiently high. Then, a dynamic calculation can be avoided and an amplification factor will suffice to account for resonance. For Solar Chimneys the smallest natural frequency n_1 is typically a beam mode in which the cross section is displaced without ovalling. A rough estimate of the frequency is:

$$n_1 > (70/H)^{0.75} \tag{2}$$

in which H is the tower height in m.

The frequency decreases as the tower height increases; it is small in number. A 1000 m - SC has a typical natural frequency of 0.17 Hz. However, the decreasing pressure correlation over the large loaded area decreases the spectrum of the modal load fluctuations considerably.

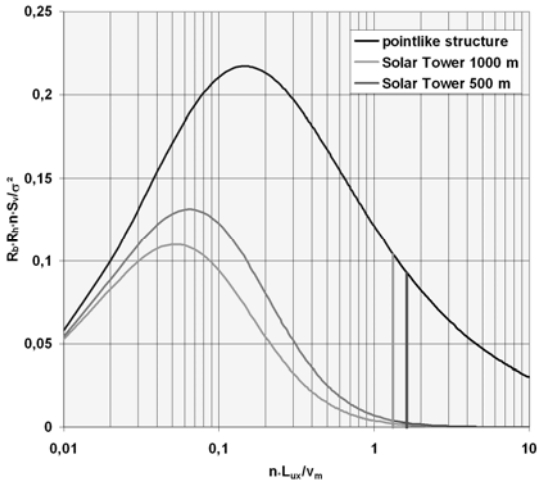

Figure 5: Spectral decomposition of the modal wind load (1st mode) for small and large loaded area.

This applies particularly in the range of the upper frequencies as may be seen in fig. 5. Clearly, most of the turbulent energy is transmitted outside the range of resonance just quasi-statically.

4.3 Fluctuating wind load

The rms-pressure fluctuations and their correlations are the basis to calculate the quasi-static shell stresses induced by turbulence. This approach – called co-variance method [Niemann et al 1996], – relies on statistical averages obtained from measured time series rather than on the time series itselves. It is preferred here instead of calculating the response in the time domain. Experimental results from full-scale measurements and wind tunnel tests may be summarized as follows:

(1) The pressure standard deviation σ_p, is proportional to the turbulence intensity I_v. At stagnation, the coefficient of σ_p / q_m (q_m designates the stagnation pressure of the mean wind speed) is $\sigma_p(z,0) / q_m(z) = 1.8\ I_v(z)$, where z is the height above the ground. As Fig. 6 shows, the intensity of pressure fluctuations varies along the circumference: it is constant before separation and drops to 50% in the wake.

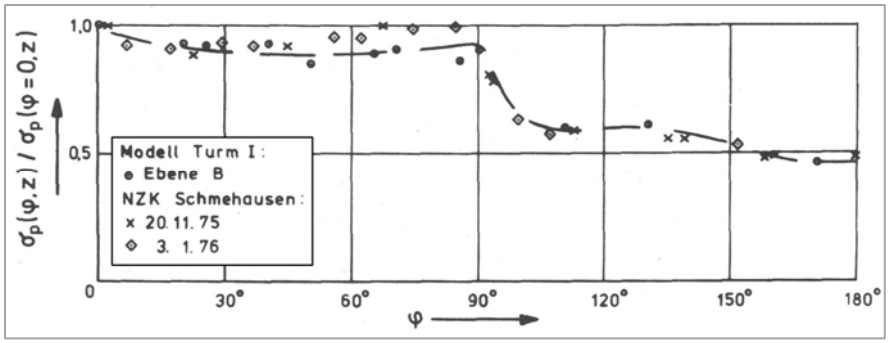

Figure 6: Summary of RMS-pressure distributions referred to the value at stagnation; at level z from the ground; from full-scale and wind tunnel experiments.

(2) Furthermore, correlation matrices were developed for current calculations which are based on wind tunnel and full-scale tests. Fig. 7a shows pressure correlations along the circumference for various reference points.

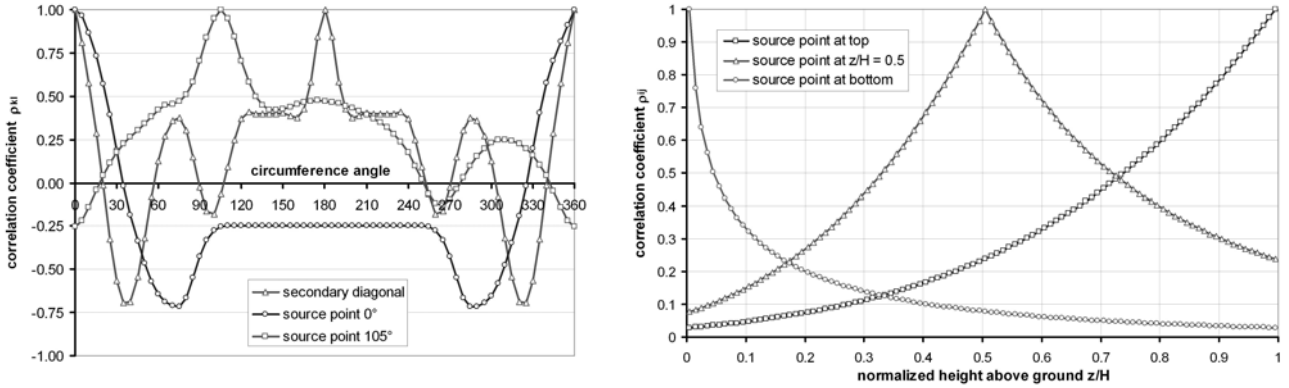

Figure 7: a) Pressure correlation around the circumference for various reference points; b) Pressure correlation along the meridians

It is interesting to see that the correlation between the stagnation point and the circumference reflects the mean pressure distribution: stagnation and maximum suction have strong negative correlation. The stagnation and the wake area have small negative correlations.

(3) The vertical correlation of pressures at two levels z_1 and z_2 along a meridian depends primarily on the correlation of turbulence. It is usually based on the integral length scale $L_{uz}(z_m)$ at the intermediate level $z_m = (z_1 - z_2)/2$:

$$\rho_z = \exp\left((z_1 - z_2) / L_{uz}(z_m)\right) \tag{3}$$

All these observation affect directly the magnitude of the response to turbulence.

4.4 Equivalent static wind pressures

The gust response was calculated based on the preceding load data for the 1000 m tower depicted in fig. 1. For the meridional tension at the tower base, the resulting quasi static gust response factor becomes 1.30, a comparatively small value. The resonant response is represented by a dynamic amplification factor of $\varphi = 1.1$, meaning that the tower is dynamically insensitive. For preliminary design calculations, the three loading components may be summarized in terms of equivalent wind pressures as follows:

$$p(z,\Theta) = \varphi \cdot \left(1 + 4.5 I_v(z)\right) \cdot q_m(z) \cdot C_p(z,\Theta) \tag{4}$$

These equivalent loads are only preliminary. A number of issues have to be clarified for final design

calculations. In particular, wind tunnel investigations are required regarding the tip effect and the pressure correlations along the meridians and the circumference. Further loading cases have to be specified for other leading stresses such as local shell bending and meridional tension at other levels than the tower base. Furthermore, the structure may still be optimized with regard to the number, stiffness, and placement of the ring beams, with regard to the diameter, and the shape of the meridian. In a close cooperation between wind and structural engineers, more options for increasing the economic feasibility of this promising technology will be detected.

5. STRUCTURAL BEHAVIOUR AND STRATEGIES OF OPTIMIZATION

From the structural point of view, solar towers are very high and slender circular cylinders, whose lower part usually turns into a hyperboloid. Indeed, the use of the double-curvature surface allows applying the benefits of shape strengthening. Because of their high slenderness, solar chimneys are a sort of huge cantilever beams. The stiffening rings along the tower help to provide this useful beam-like behaviour, as well as increase the buckling stiffness.

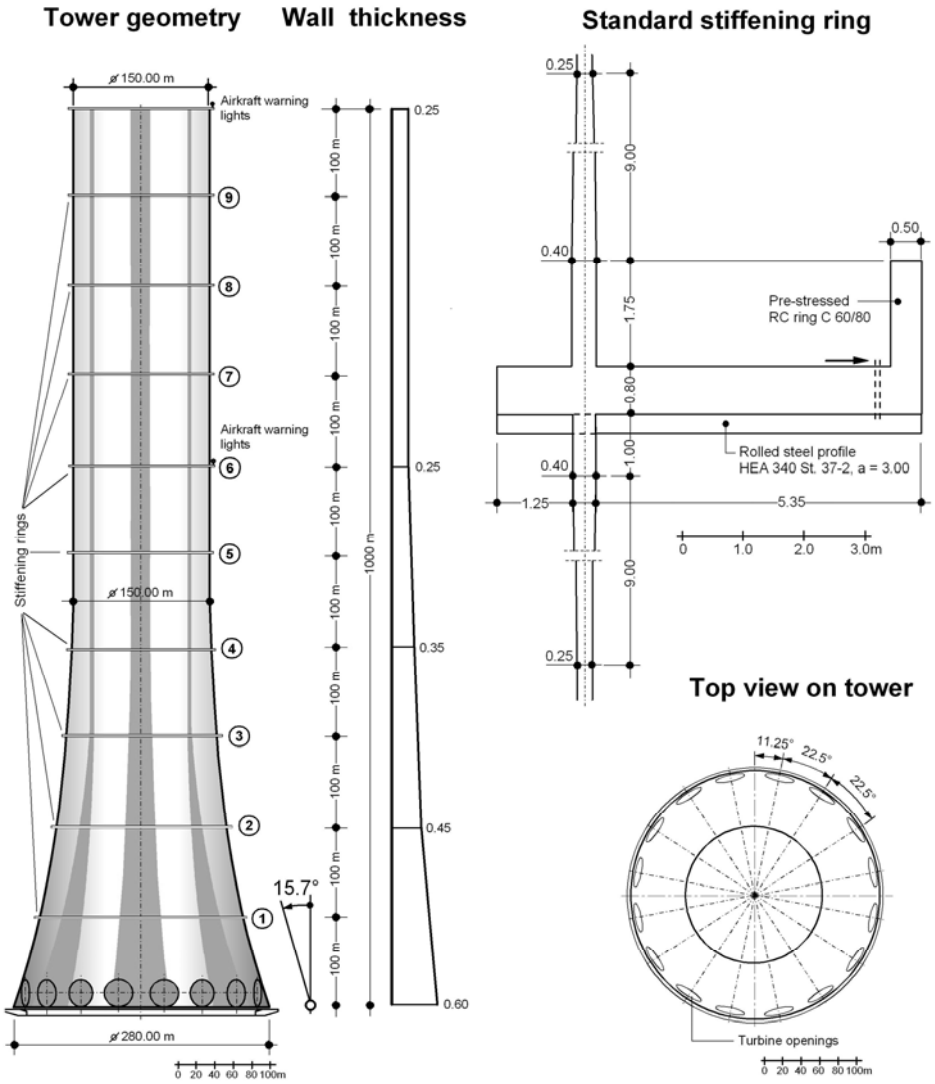

Figure 8: 1000m solar chimney (courtesy of Krätzig & Partner, Bochum)

Figure 8 shows the structural components of a solar chimney. Both the tower and the stiffening rings are made of reinforced concrete. Stiffening rings may be pre-stressed.

The design of such a thin, concrete shell is affected by various questions. On one hand, high

compressive stresses and buckling are faced by high strength concrete (design calculations usually refer to C 50/60) and an appropriate distribution of thickness. On the other hand, tension in the shell, caused by variable actions such as wind, should be avoided in order to make the most of the material properties and save reinforcement. In all of that, stiffening rings play an important role, but even if they are needed because of structural issues, difficulties due to their construction cannot be ignored in a good design of the solar tower. Therefore, the question of optimization of the tower regarding the number, stiffness, and placement of the ring beams must be investigated, in order to find the best compromise between structural needs and economical constraints. Furthermore, the structure may be optimized with regard to the diameter and the shape of the meridian.

Figure 9 shows the behaviour of the 1000m-SC with ten stiffening rings at a spacing of 100 meters under wind and dead load, in terms of internal force in the meridional direction. At the ultimate limit states wind loading is multiplied by the partial safety factor 1.6 (according to VGB-650 Ue), while self weight is not amplified if favourable. The lower part of the tower is the most sensitive to wind action, since self weight is not enough to cover meridional forces of tension. Local compressions due to wind are present at the upper levels of the tower height, probably due to a shell-like behaviour. But no advantage is provided in terms of saving reinforcement, since tension must be somewhere else at the same level because of equilibrium.

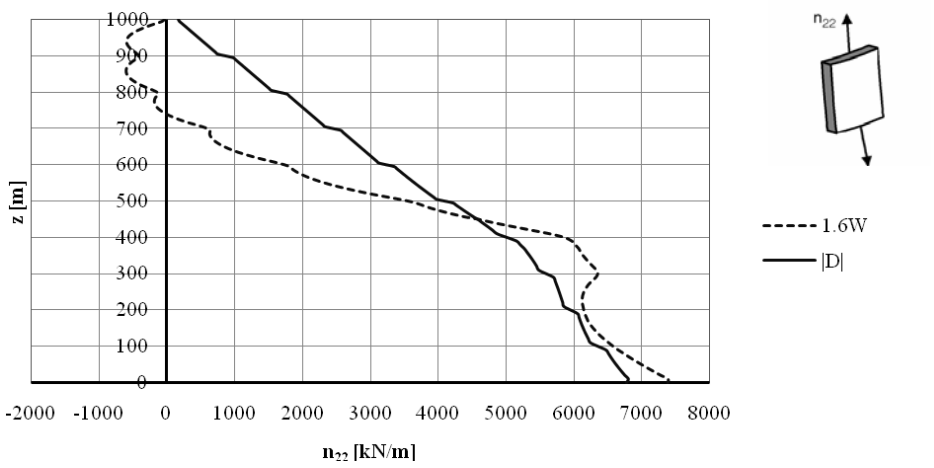

Figure 9: Meridional force at stagnation resulting from wind and dead load

A strategy of optimization of such a structure in view of the meridional tension in the shell may be to increase the stiffness of the ring beams and, because of economical reasons, reduce their number. For preliminary calculations and comparisons between different models, the stiffness of the rings can be easily increased just increasing the Young Modulus of the material. Then, the possibility to achieve such a stiffness (especially bending stiffness to prevent shell deformations) shall be investigated. For example, the dimensions of the cross section of the rings can be increased, and pre-stressing is an option as well.

Increase of stiffness of the ring beams in the cylindrical part of the chimney provides benefits in the lower, most sensitive, part of the tower height. Instead, increase of stiffness at lower levels may be unnecessary, thanks to the benefits of shape, given by the double-curvature surface. All of that should be observed in figure 10, showing the circumferential distribution of the meridional force caused by wind at a representative critical level of the tower (350 m). The continuous line in the graph refers to the 1000m-SC with ten stiffening rings and standard value of ring stiffness, while the dotted and dashed lines are associated to the same structure but with an increase in stiffness (3 times) of some rings (the upper five rings and all of them, respectively). The discontinuous lines depart from the continuous one, with a significant reduction of tension at the windward side. But the dotted and the dashed lines are very similar; this indicates that the contribution of the lower rings is less important.

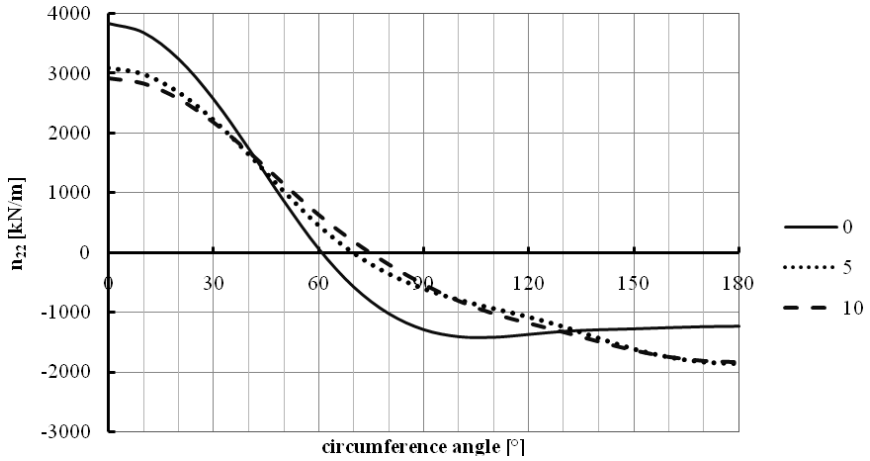

Figure 10: Circumferential distribution of the meridional force caused by wind at a representative critical level (350 m), SC with 10 stiffening rings. The legend stands for the number of ring beams from the top whose stiffness has been increased (3 times).

A bigger benefit is also achieved if the partial safety factor for wind loading is reduced. Figure 11 refers to a critical level of the solar tower with ten stiffening rings at a spacing of 100 meters. It shows that a reduction of the partial safety factor avoids tension in the meridional direction even without increasing the stiffness of the ring beams.

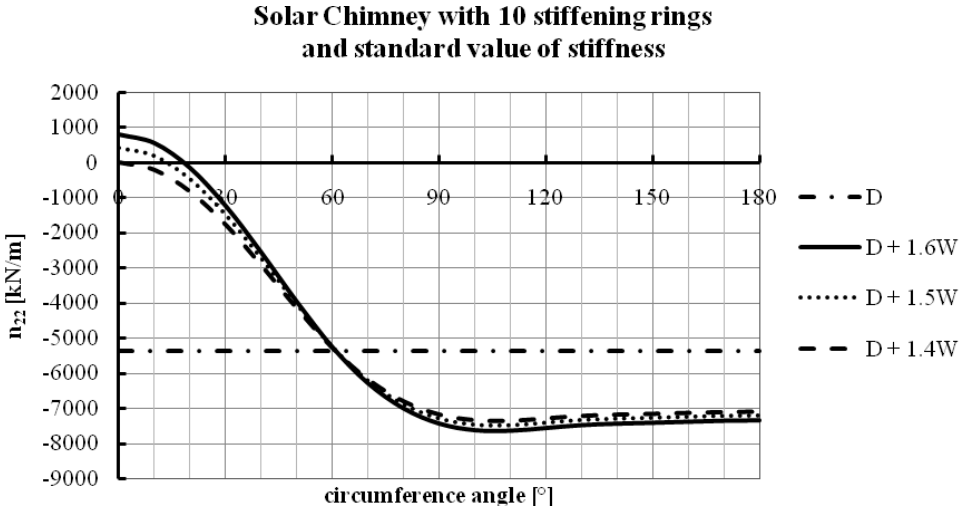

Figure 11: Stresses resulting from wind and dead load at a representative critical level (350m), solar chimney with 10 stiffening rings.

A combined strategy that includes both an increase in stiffness of the rings and a reduction of the partial safety factor allows achieving equally good results even with a smaller number of stiffening rings. The comparison between figures 11 and 12 shows that. Both figures represent the circumferential distribution of the meridional force at a critical level for different values of the partial safety factor for wind loading, but they differ in the number and stiffness of the ring beams (ten rings with standard stiffness and seven rings with doubled stiffness, respectively). It can be seen that the graphs are very similar.

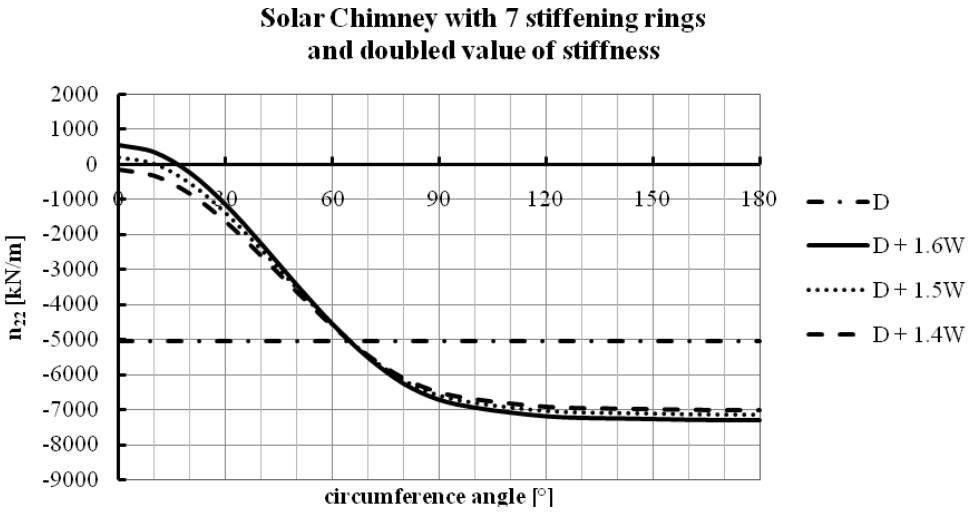

Figure 12: Stresses resulting from wind and dead load at a representative critical level (350m), solar chimney with 7 stiffening rings.

Relying on these preliminary results, the design of the solar chimney aims at building the tower with the minimum percentage of steel needed. According to the VGB guideline, it is 0.3% in the meridional direction and 0.3% and 0.4% in the circumferential direction, in the lower and upper half respectively. Accordingly, the minimum amount of reinforcement for the 1000m-SC in the meridional direction is 4720 tons, which has to be increased by approximately 10% to account for overlapping.

1000m-SC, 10 Stiffening rings at a spacing of 100 m			
	Value of stiffness	Amount of meridional steel [tons]	Design based on the minimum shell reinforcement
D + 1.6W	standard	5202	no
D + 1.5W	standard	4730	no
D + 1.4W	standard	4720	yes

Table 2: Tower with 10 stiffening rings, amount of meridional reinforcement (local bending of stiffening rings not included)

There are several options to achieve the goal of minimizing the amount of required reinforcement. Table 2 quantifies the influence of the partial safety factor, with standard number and stiffness of the ring beams. It may be concluded that if an increase in stiffness of the ring beams has to be avoided, at least ten rings are needed and the partial safety factor applied to the wind action should be reduced to 1.4, in order to reduce the amount of steel needed in the meridional direction to its minimum. The second option to reduce the required reinforcement is depicted in table 3: the results refer to 7 ring beams with standard, doubled and tripled stiffness. The table shows that for the partial wind load factor of 1.6 of the VGB-guideline, the minimum reinforcement can only be achieved by a tripled stiffness. However, this is rather unrealistic with the ring beams considered in this study. For double ring stiffness and 7 ring beams in the upper part, the minimum reinforcement is achieved with a partial wind load safety factor of 1.5. In practical terms, with a rough calculation which takes into account an increase of steel because of bending moments and overlapping (approximately 20% more), the total amount of shell reinforcement, i.e. in the meridional and in the circumferential direction, results around 12000 tons, which related to the volume of concrete of approximately 200,000 m^3, provides a rather low degree of reinforcement of 60 kg/m^3.

1000m-SC, 7 Stiffening rings (placed at 160-300-440-580-720-860-1000 m)			
	Value of stiffness	Amount of meridional steel [tons]	Design based on the minimum shell reinforcement
D + 1.6W	standard	9598	no
	doubled	4934	no
	tripled	4720	yes
D + 1.5W	standard	6998	no
	doubled	4720	yes
	tripled	4720	yes
D + 1.4W	standard	5503	no
	doubled	4720	yes
	tripled	4720	yes

Table 3: Tower with 7 stiffening rings, amount of meridional reinforcement (local bending of stiffening rings not included)

These numbers are only indicative. They need further detailed calculations. The aim of the study was to explore the possibilities of reducing the amount of reinforcement by optimizing the structural behavior of a typical tower. Stiffening rings, their number and stiffness as well as an improved partial safety factor for the wind load are effective in achieving this goal.

REFERENCES

Niemann H.-J., Flaga A., Höffer R., Hölscher N., Kasperski M. (1996). "Structural response to wind" In: Dynamics of Civil Engineering Structures, Wilfried B. Krätzig & Hans-Jürgen Niemann (Eds.) A.A. Balkema, Rotterdam.

von Backström Th. W., Harte R., Höffer R., Krätzig W.B., Kröger D.G., Niemann H.-J., van Zijl G.P.A.G. (2008). "State and Recent Advances in Research and Design of Solar Chimney Power Plant Technology", VGB PowerTech 88, 64-71.

Busch D., Harte R., Krätzig W.B., Montag U. (2002). "New Natural Draft Cooling Tower of 200m of height", Journ. Engineering Structures 22, 2002.

Graffmann M., Harte R., Krätzig W.B., Montag U. (2007). "Sturmbean-spruchte dünne Stahlbetonschalen im Ingenieurbau", in: P. Mark, M. Strack (Eds.), Fünf Jahre in Forschung, Lehre und Praxis, 183-195, Ruhr-University Bochum.

Gould Ph.L., Krätzig W.B. (2004). "Cooling Tower Structures", in: W.-F. Chen, E.M. Lui (eds.), Handbook of Structural Engineering, 27/1-41, CRC Press, Boca Raton.

Günther H. (1931). "In hundert Jahren - Die künftige Energieversorgung der Welt (In hundred years - Future energy supply of the world)". Kosmos, Franckh'sche Verlagshandlung Stuttgart.

Schlaich J., Bergermann R., Schiel W., Weinrebe G. (2005). "Design of Commercial Solar Updraft Tower Systems", Journ of Solar Energy Engineering, 127, 117-124.

Pretorius J.P., Kröger D.G. (2007). "Sensitivity Analysis of the Operating and Technical Specifications of a SCPP", ASME Journ. of Solar Energy Engg. 129, 171-178.

Pretorius J.P. (2007), "Optimization and Control of a Large-Scale SCPP". Ph.D. thesis, University of Stellenbosch.

Pretorius J.P., Kröger D.G. (2006). "Solar Chimney Power Plant Performance", ASME Journ. of Solar Energy Engg. 128, 302-311.

Schlaich J. (1995). "The Solar Chimney, Electricity from the Sun", Edition A. Menges, Stuttgart, Germany.

Niemann H.-J., Hölscher N., Meiswinkel R. (2007) "A probabilistic approach for the determination of extreme actions with respect to the structural design", Proc. of ICAPP 2007, Nice, France.

Bradbury W.M.S., Deaves D.M., Hunt J.C.R., Kershaw R., Nakamura K., Hardman M.E., and Bearman P.W. (1994). "The importance of convective gusts", Meteorological Applications, 1, 365-378.

Lupi F., (2009). "Structural behaviour, optimization and design of a solar chimney prototype under wind loading and other actions". Tesi di laurea, Università degli Studi di Firenze – Ruhr Universitaet Bochum

VGB-610 Ue, (2005). "Structural Design of Cooling Towers, Technical Guideline for the Structural Design, Computation, and Execution of Cooling Towers", VGB Kraftwerks-technik, Germany, Essen.

EN 1990:2001-11, (2001). "Eurocode - Basis of structural design", CEN.